

Rapid proton transfer under flashing light at both functional sides of dark-adapted Photosystem II particles

Oliver Bögershausen, Wolfgang Junge *

Abt. Biophysik, FB Biologie / Chemie, Universität Osnabrück, D-49069 Osnabrück, Germany

Received 24 December 1994; revised 17 March 1995; accepted 3 April 1995

Abstract

By exposing dark-adapted Photosystem II core particles to a series of light flashes, we aimed at kinetic resolution of proton release during the four steps of water oxidation. The signal-to-noise ratio was improved by averaging under repetitive dark adaptation. The previously observed kinetic damping of pH-transients by particle aggregation was prevented by detergent. The complicating superimposition of protolytic events at the donor side (water oxidation) and at the acceptor side (quinone oxido-reduction) was unravelled by characterizing the rate constants of electron and proton transfer at the acceptor side ($Q_A^- \cdot nH^+ + DCBQ \rightarrow Q_A + DCBQ^- + nH^+$; $k = 1.7 \cdot 10^6 \text{ M}^{-1} \text{ s}^{-1}$ // $2 DCBQ^- + 2H^+ \rightarrow DCBQ + DCBQH_2$; $k = 4 \cdot 10^8 \text{ M}^{-1} \text{ s}^{-1}$). Contrasting with the pronounced period of four oscillations of the oxygen-evolving centre, the extent of proton release was practically constant. The apparent half-rise time of the stepped acidification was shortened upon lowering of the pH (250 μs at pH 7.5, 70 μs at pH 6.0 and 12 μs at pH 5.2). This kinetic behaviour was independent of the nature and the concentration of the added pH-indicator. We conclude that this reflects the protolysis of several electrostatically interacting acids at the surface of the protein in response to a new positive charge on Y_Z^+ , and persisting upon electron transfer from the manganese cluster to Y_Z^+ .

Keywords: Photosynthesis; Photosystem II; Core particle; Water oxidation; Oxygen evolution; Electron transfer; Proton transfer; Dark adaptation, repetitive

1. Introduction

One molecule of dioxygen and four protons are the products of the oxidation of two molecules of water. Photosystem II of cyanobacteria and green plants uses four quanta of light (double arrows) to drive its catalytic manganese cluster through a series of redox states, $S_0 \Rightarrow S_1 \Rightarrow S_2 \Rightarrow S_3 \Rightarrow S_4 \rightarrow S_0$. Oxygen is evolved only during the last transition, $S_3 \Rightarrow S_4 \rightarrow S_0$ (see [1,2] for recent reviews). Contrastingly, proton release is distributed over all four transitions with large variations of the pattern depending on the material (thylakoids [3], PS-II-enriched membranes [4] and core particles [5–7]) and the pH (see [8] for a review). It is of great interest to know whether or not the

observed release of protons is just a peripheral event, e.g., an electrostatic response of remote amino acids to the deposition of positive charges in the catalytic centre, or diagnostic of partial reactions in the catalytic centre itself. Detailed schemes for the deprotonation of bound water (derivatives) during the four redox steps have been hypothesized (e.g., [9]). There are at least three strong arguments in favour of a peripheral origin of the observed proton release: (1) the major portion of proton release can be faster than the electron transfer from the manganese cluster to Y_Z^+ [3]; (2) the pattern of proton release greatly varies as function of the pH and the material without similar variation of the rates [10] and the stepping of the redox reactions [7]; (3) variations of the pattern of proton release do not affect the pattern of local electrochromism [10].

The least featured pattern of proton release has been observed in isolated PS II core particles. It progresses about 1:1:1:1 for transitions $S_0 \Rightarrow S_1 \Rightarrow S_2 \Rightarrow S_3 \Rightarrow S_{4,0}$ [5–7] in core preparations from spinach and pea prepared after Ghanotakis et al. [11] and Haag et al. [12], respectively. The same holds true [10,13] for another type of a core preparation from pea prepared after the procedure by

Abbreviations: β -DM, *n*-dodecyl β -D-maltoside; BCP, bromocresol purple; Bis-Tris, bis(2-hydroxyethyl)iminotris(hydroxymethyl)methane; Chl, chlorophyll; CR, cresol red; DCBQ, 2,5-dichloro-*p*-benzoquinone; fwhm, full width at half maximum; Mes, 2-*N*-morpholinoethanesulfonic acid; MR, Methyl red; PR, Phenol red; PS II, Photosystem II; Q_A , primary quinone acceptor of PS II; Y_Z , tyrosine 161 on PS II subunit D1.

* Corresponding author. E-mail: junge@sfb.biologie.uni-osnabrueck.de. Fax: +49 541 9692870.

Van Leeuwen et al. [14]. Whereas particle aggregation in the first preparation [11] delayed the response of pH-indicating dyes to supposedly rapid events at the protein surface (into the range of 100 ms), rapid pH-transients (10 μ s) have been observed in the last one. A rigorous understanding of the kinetic behaviour in this material, however, has to cope with four obstacles, namely (a) the more rapid relaxation of higher oxidation states of the manganese cluster as compared to thylakoids and PS-II-enriched membrane fragments, (b) the remaining aggregation of core particles, (c) the superimposition of protolytic events at both sides of PS II, and (d) the dependence of the rates of proton transfer on the nature and the concentration of the pH-indicating dyes. These properties are scrutinized in this article.

2. Materials and methods

Photosystem II core particles were prepared according to Van Leeuwen et al. [14] but from 10–12-day-old pea seedlings, not from spinach. We started from PS-II-enriched membrane fragments [15] prepared according to Lübbbers and Junge [5], but the last washing step and the resuspension were modified and carried out in buffer A (20 mM Bis-Tris/HCl, 400 mM sucrose, 20 mM MgCl₂, 5 mM CaCl₂, 10 mM MgSO₄, 0.03% (w/v) β -DM), at pH 6.5. Concentrated core particles were stored at -80° C until use. The specific oxygen-evolving activity of these core particles varied between 1200 and 1800 μ mol O₂ / (mg Chl \cdot h) in buffer A. It was determined with a Clark-type electrode under continuous light with DCBQ as artificial electron acceptor.

Flash-spectrophotometric measurements were performed as described elsewhere [16]. The sample was excited with saturating flashes provided by a Xenon lamp (10 μ s fwhm, Schott RG 610). The transient signals were averaged (Nicolet Pro30), stored and analysed on a Micro Vax.

Three different regimes of flash excitation were applied. (i) *Long-term dark adaptation*: Samples were kept 20 min in darkness and then excited with only one flash group per sample. (ii) *Repetitive dark adaptation*: A sample was excited repetitively with up to 20 flash groups separated by 25 s intervals of darkness. (iii) *Repetitive excitation*: A sample was excited up to 100 times with a repetition rate > 1 Hz.

Proton release was measured spectrophotometrically by absorption changes of the hydrophilic dyes Bromocresol purple (BCP: wavelength 575 nm, pH range 5.5–7.2), Cresol red (CR: 575 nm, pH range 7.0–8.2), Phenol red (PR: 560 nm, pH range 6.2–8.2), and Methyl red (MR: 560 nm, pH range 5.2–6.0). At wavelengths of 575 or 560 nm the superimposition of intrinsic signals to the pH-response of added dyes was negligible (see Fig. 5B, upper trace). pH transients were recorded with samples in the

absence of buffer. The buffer was removed by gel filtration (PD-10, Pharmacia). The elution medium contained 5 mM CaCl₂, 5 mM MgCl₂, 0.01% β -DM (medium I). The gel-filtration procedure impaired neither oxygen evolution under continuous light nor the pattern of UV-absorption transients under flashing light (not documented). For spectrophotometry the sample was diluted to yield a chlorophyll concentration of 2 μ M. 0.1 mM DCBQ and 0.2 mM hexacyanoferrate(III) were added as electron acceptors, with the latter preventing the protonation which follows the slow dismutation of the semiquinone form of DCBQ ($k = 6.3 \cdot 10^8$ M⁻¹ s⁻¹ [17]). Measurements of the pH- and detergent-dependence of the rate of proton release were performed in the repetitive excitation mode (1.25 Hz). The electrical bandwidth was 100 kHz at pH ≤ 6 and 30 kHz at pH > 6 . The time per address of the digitizer was 10 μ s. The optical pathlength was 2 cm.

For the investigations in the UV at 295 nm, the sample was diluted in medium I to 8 μ M Chl without gel filtration. DCBQ served as artificial electron acceptor. Hexacyanoferrate(III) was omitted because of its high optical absorbance at this wavelength. The Kok parameter triple (misses, double hits, and the population of S₁) was determined based on UV-absorption transients at 295 nm. These transients are attributed mainly to the oxidoreduction of manganese [18]. A component with millisecond half-decay time which is most pronounced on the third flash (as is oxygen liberation) has been attributed to the oxygen-evolving transition S₃ \Rightarrow S₄ \rightarrow S₀ [19]. The sum of the extents at 295 nm of this millisecond component over the first 6 transients was set to 100% because almost all reaction centres had then passed through the oxygen-evolving step, even when considering the large probability of misses (about 20%). Due to the small probability of double hits, a second S₃ \Rightarrow S_{4,0} transient was not expected before the 7th flash. The pattern was deconvoluted by a home-made routine to yield the three Kok parameters. Absorption transients at 295 nm were measured both with long-term dark-adapted samples and under repetitive dark adaptation. 100 transients were averaged with an electrical bandwidth of 3 kHz and 50 μ s per address. A cell with 1 cm optical pathlength was used for measurements in the UV (295, 320 nm).

Exponential fits to kinetic data were performed with the plotdata routine (J.L. Chuma, TRIUMF, University of Vancouver, Canada) and kinetic simulations were carried out by using Mathcad 5.0 (MathSoft, Cambridge, MA, USA).

3. Results

3.1. Repetitive dark adaptation is equivalent to long-term dark adaptation

We checked whether the synchronization of oxygen evolution as a function of flash number was the same

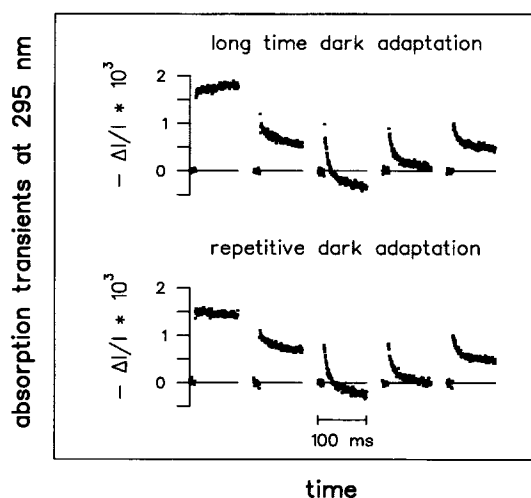


Fig. 1. UV absorption transients at 295 nm. The upper trace resulted from a long-term dark-adapted sample (20 min) and the lower trace from a repetitively dark-adapted one (25 s interval between flash series). Conditions: pH 6.0, 50 μ s per address (only every 10th data point is displayed), 100 ms between consecutive flashes in a series, DCBQ (0.1 mM) as electron acceptor, 100 transients averaged.

under long-term (20 min) and repetitive dark adaptation (25 s). The extent of the millisecond and of the stable components of the absorption transients at 295 nm was determined as function of the flash number. The millisecond phase reflects the oxygen-evolving step $S_3 \Rightarrow S_{4,0}$ and thereby a reliable measure of the progression through $S_i \Rightarrow S_{i+1}$ [20–23]. The results are given in Fig. 1 and Fig. 2. Fig. 1 shows the original traces resulting from measurements under the two different regimes of dark adaptation. The half-decay time of the ms component was 4.5 ms, the same as published by Van Leeuwen et al. [23]. The oscillations of both the millisecond and the stable component were almost the same under the two conditions of dark adaptation (Fig. 2A and B). A fit (solid line in Fig. 2A) yielded the Kok parameter triple as given in Table 1. Repetitive dark adaptation was therefore equivalent to long-term dark adaptation. Oscillations with period four were clearly expressed, although strongly dampened.

A minor offset was observed on every flash at 295 nm. It was absent in the presence of hexacyanoferrate(III) (not documented) and therefore attributed to changes at the acceptor side of PS II. State S_0 has been reported to decay with a half-rise time of 2–3 min in the original preparation from spinach of Van Leeuwen et al. [23] as the starting material. If the same holds true in our preparation, which was based on pea leaves, we expected a starting population of 80% S_1 and 20% S_0 under repetitive dark adaptation. The broken line in Fig. 2A shows the then expected behaviour (calculated with the same probabilities of misses and double hits as before). This fit was inferior to the one based on 100% S_1 . Accordingly, the relaxation of state S_0 in our preparation occurred in a shorter time than the interval of 25 s between groups of flashes.

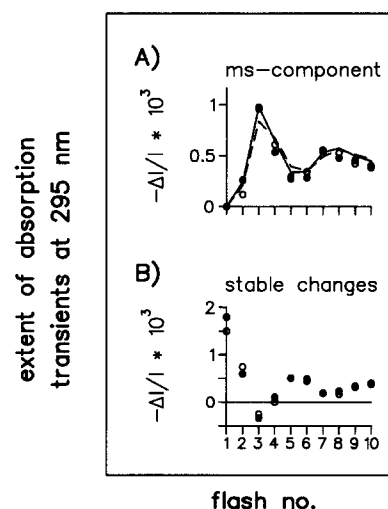


Fig. 2. The extents of the ms component and the stable step of absorption transients at 295 nm as function of the flash number based on original data as given in Fig. 1. (A) The extent of the millisecond component which is indicative of the $S_3 \Rightarrow S_{4,0}$ transition. Closed cycles: long-term dark-adapted, open cycles: repetitively dark-adapted sample. Line: A fit of the data of the long-term dark-adapted sample using the Kok parameters given in Table 1. Broken line: Alternative fit with 80% S_1 and 20% S_0 instead of 100% S_1 . (B) The extent of the stable absorption changes after each flash (symbols are the same as in (A)).

3.2. The pattern of proton release in repetitively dark-adapted material

The extent of proton release was measured as function of flash number in *repetitively dark-adapted material*. We observed only a very weak oscillation, not only at pH 6.3 as documented in Fig. 3 but also at pH 5 and 7 (not documented). The rates of proton release were the same within error limits for every oxidation step. However, they were strongly dependent on the pH (see below). In *long-term dark-adapted material* we observed essentially the same extents and rates with the exception of the first flash (see further down). When the original pH-transients as function of the flash number (see Fig. 3) were deconvoluted in terms of the independently determined Kok parameter triple (at pH 6.3: misses 20%, double hits 5% and

Table 1
Kok parameter triples

pH		S_1	α	β
6.0	*	100%	23.1%	7%
6.0	**	100%	23.3%	6%
5.0	**	82%	26.1%	2%
5.5	**	91%	22.8%	4%
6.5	**	100%	21.6%	5%
7.0	**	86%	21.5%	7%

S-state distribution and probabilities of misses (α) and double hits (β) of the core particles as function of pH and regime of dark adaptation (long-term dark adaptation *; repetitive dark adaptation **). All data were deduced from the millisecond component of the transients at 295 nm (see Figs. 1 and 2). S_2 and S_3 were set to 0.

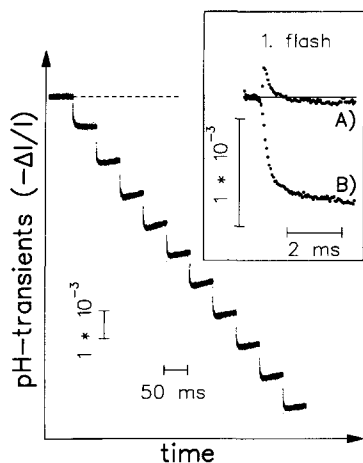


Fig. 3. Original pH-transients under excitation of core particles with a series of 10 flashes of light. Repetitive dark adaptation (pH 6.3), Bromocresol purple (30 μ M). Inset: The pH-transient on the first flash at expanded time scale, (A) under long-term dark adaptation and (B) under repetitive dark adaptation. DCBQ (0.1 mM) and hexacyanoferrate(III) (0.2 mM) as electron acceptors, up to 100 signals averaged.

100% S_1) the oscillation of proton release as function of the transitions $S_i \Rightarrow S_{i+1}$ was still small, namely 1.0:0.8:1.1:1.1 starting with $S_0 \Rightarrow S_1$.

3.3. Long-term dark adaptation causes extra proton uptake upon the first flash

The absence of large oscillations of proton release has already been inferred from studies on other types of core particle preparation [5,6]. However, in these studies the analysis was less clear due to the superimposed proton uptake at the acceptor side of PS II upon the first flash. We found the same complication in our material under long-term dark adaptation when using hexacyanoferrate(III) (see also reaction scheme in [24]). The inset of Fig. 3 shows pH transients upon the first flash under long-term (trace A) and under repetitive dark adaptation (trace B). In (A) stable proton release was apparently absent on the first flash. But there was a rapid transient of proton uptake. This became more pronounced at basic pH (see Fig. 5C), where the rate of proton release was slowed down (see below). Whether or not there was a contribution of inactive centres to the acid/base reaction upon the first flash under long-term dark adaptation (see e.g., [25]) cannot be decided.

3.4. Kinetic properties of the pH transients

The PS II core particles used in this work showed a very rapid acidification of the medium. We investigated two parameters affecting the rate: (i) The detergent concentration which bears on the aggregation state of core particles and (ii) the pH. The rise of the acidification was

always biphasic. It was analysed in terms of two exponentials.

The concentration of the detergent β -DM in the medium was varied from 0 to 0.09% (w/v). The minimal concentration of β -DM was about $5 \cdot 10^{-5}$ % (w/v) after dilution of the core particles stored in medium I after gel filtration. Fig. 4A shows pH-transients under repetitive excitation in three experiments with 0.003, 0.004, 0.005% (w/v) β -DM added. The increase of the detergent concentration accelerated the acidification. Both the rate constant of the fast component and the relative extents of the two components were affected. The proportion of the fast component increased from 15% at 0.003% to 70% at 0.005% (w/v) β -DM. The rate constant of the fast component increased from 3 ms^{-1} to 10 ms^{-1} when the detergent concentration was raised from 0.003% to 0.01% (w/v). At higher concentration there was no further acceleration (Fig. 4B). At concentrations lower than 0.003% (w/v) the kinetic behaviour was more complex.

One residual slow component of about 30% (at pH 6.2) remained even at high detergent concentration. We asked whether this was attributable to events at the acceptor side of PS II. Let us first expound the rationale underlying the experiments. According to the literature, the second quinone, Q_B , is absent from this preparation [23] (see also [26]). The reduction of Q_A to yield Q_A^- causes fractional

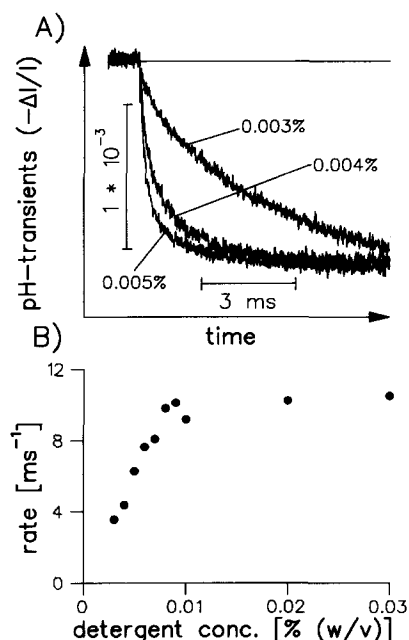


Fig. 4. Influence of the detergent concentration on the kinetics of pH-transients in repetitively excited core particles as monitored by absorption changes of Bromocresol purple. (A) Three original traces obtained with different detergent concentrations, upper 0.003%, middle 0.004%, and lower 0.005% (w/v) β -DM. (B) The dependence of the rate constant of the fast acidification on the detergent concentration. The proportion of the fast component was also strongly dependent on the detergent concentration. At 0.003% β -DM it was only 15%. Conditions: pH 6.2, 10 μ s per address, 50 signals averaged, repetitive excitation.

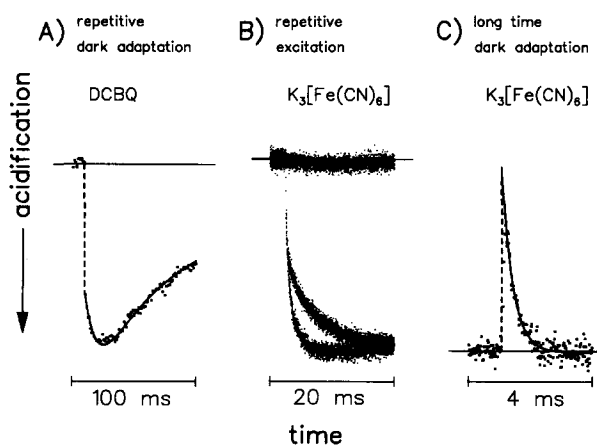


Fig. 5. The superimposition of protonation and deprotonation at the acceptor and the donor side of PSII. (A) shows the original trace (dots) and a simulation (solid line) of the superimposition of the protonic events at both sides of PS II with DCBQ as electron acceptor (see text). Three different components are apparent: A rapid and a slow acidification followed by an even slower alkalization. pH 5.5, 0.1 mM DCBQ, first flash, repetitive dark adaptation, 30 μ M MR, 560 nm. (B) The influence of the concentration of the electron acceptor hexacyanoferrate(III) (0.1 mM and 2.0 mM) on the rate of the slow component of the net acidification. Higher acceptor concentration accelerated the slow component of the acidification. The upper trace was obtained with 10 mM buffer (Mes). The absence of any transient demonstrated the pH-indicating nature of all signal components at this wavelength. The lower traces were obtained in the absence of buffer with 0.1 and 2.0 mM hexacyanoferrate(III) at pH 5.5. Repetitive excitation, 50 μ M BCP, 575 nm. (C) Transient proton uptake upon the first flash in a long-term dark-adapted sample with hexacyanoferrate(III) as electron acceptor (dots: original data; solid line: fit), pH 7.4, 0.2 mM hexacyanoferrate(III), first flash, long-term dark adaptation, 20 μ M PR, 560 nm.

proton uptake into the protein moiety surrounding the quinone binding pocket to yield $Q_A^- \cdot nH^+$ (see also [27]). In the presence of an artificial electron acceptor, which reacts directly with Q_A^- but does not bind a proton upon reduction, proton uptake is reversed. The rapid uptake of protons when Q_A is reduced and their slower release upon further electron transfer to an artificial electron acceptor diminishes the extent of the *rapid* acidification and instead produces a slow component but yields the same total magnitude as expected without this complication. If this interpretation is correct, the rate of the residual slow acidification is expected to increase with the concentration of the non-proton-binding electron acceptor. It should simply follow the rate of its bimolecular reaction with Q_A^- . This was checked using two different electron acceptors, namely hexacyanoferrate(III) and DCBQ.

Fig. 5B shows pH-transients under repetitive excitation for two concentrations of hexacyanoferrate(III), and one trace in strongly buffered suspension as a control. The slow phase (about 45% in both measurements, pH 5.5) of the net acidification was accelerated by increasing the concentration of hexacyanoferrate(III). This result was in line with the above notion that the slow phase reflected the deprotonation of $Q_A^- \cdot nH^+$ upon electron transfer to hexa-

cyanoferrate(III). This behaviour was even more obvious when using DCBQ, an electron acceptor which does not bind a proton upon formation of its semiquinone stage, $DCBQ^-$, but then dismutates into DCBQ and $DCBQ^{2-}$ to yield $DCBQH_2$ [17]. The result of such an experiment is shown in Fig. 5A. A rapid acidification was then followed by a slower phase, which turned into an alkalization. We varied the concentration of DCBQ and found the rate of slow phase proportionally accelerated. This gives evidence for a bimolecular reaction between Q_A^- and DCBQ.

Fig. 5C shows the situation when proton uptake at the acceptor side of PS II is not reversed. It shows the pH transient upon the first flash in a long-term dark-adapted sample at pH 7.4 with hexacyanoferrate(III), that causes a preoxidation of the non-haem iron [28]. Its rereduction is accompanied by a *stable* proton uptake (see Discussion). The trace was obtained at pH 7.4 where proton uptake (at $Fe(III) \Rightarrow Fe(II)$) was very fast and kinetically clearly separated from the slower proton release by water oxidation. Fig. 5C shows the original trace (dots) and the fit by a single exponential (solid line). The first 100 μ s were discarded from the data used for fitting. The rate constant was 2.8 ms^{-1} , the same as determined at this pH for the rapid phase resulting from a biexponential analysis of the acidification under repetitive excitation (see below). Because of the very rapid rise and the permanence of proton

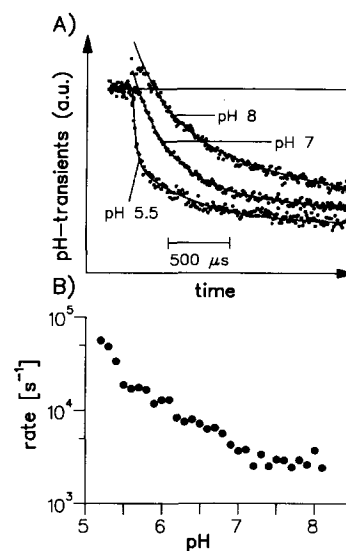


Fig. 6. The kinetics of pH-transients in core particles as function of the pH. (A) Original traces (dots) at pH 5.5, 7 and 8. The solid lines represent fits with two exponentials (at pH 5.5 for example: 54% fast with $k_f = 34 \text{ ms}^{-1}$, 46% slow with $k_s = 2 \text{ ms}^{-1}$). At pH ≥ 7 the data points of the first 70 μ s were not included in the fit-procedure. (B) The rate of the fast component as function of pH. Overlapping data points from the use of different pH-indicating dyes were coincident, namely in the pH-domain 5.5 to 6.0 resulting from using MR and BCP, in the range 6.2 to 7.2 from BCP and PR, in the range 7.0 to 7.2 from BCP, PR and CR, and in the range 7.0 to 7.6 from PR and CR. The rate was independent of the concentration of these indicator dyes (not documented). Conditions: 10 μ s per address, 60 signals averaged, repetitive mode.

uptake during the reduction of Fe(III) at the acceptor side of PS II, the rapid proton release from the donor side was directly apparent.

3.5. The pH-dependence of proton release

The pH-dependence of the rapid phase of the acidification was investigated under repetitive excitation. Fig. 6A shows original traces at pH 5.5, 7 and 8. They were analyzed in terms of two exponentials (at pH ≥ 7 the first 70 μs were discarded). Fig. 6B shows the rate constant of the rapid phase as function of the pH. Lowering of the pH accelerated the reaction. At acid pH the release of protons was more rapid than the oxidation of the manganese cluster by Y_Z^+ . The half-rise time at pH 5.2 was 12 μs . The rate increased about tenfold and proportional to the proton concentration between pH 6 and 5 according to $k_{\text{eff}} \cong k^+ \cdot [\text{H}^+]$ with $k^+ = 10^{10} \text{ M}^{-1} \text{ s}^{-1}$. This figure for k^+ is of the same order of magnitude as the diffusion controlled on-reaction for the protonation of a base in contact with bulk water. In the pH – range between 6 and 8.2 the correlation with the proton concentration became sublinear. *This kinetic behaviour was independent of the chemical nature and the concentration of the indicator dye.* The relative extents of the rapid and the slow phase were changed less dramatically; at pH 5 and 7.5 only 50% of the acidification occurred rapidly, at pH 6.5 about 80%.

4. Discussion

Four protons are produced when the oxygen-evolving complex reacts with two molecules of water to yield dioxygen. In addition, there is a transient electrostatic response, protons are released and taken up again due to the deposition and removal of oxidizing equivalents from the catalytic centre. This interplay between ‘chemical’ and ‘electrostatical (Bohr effect) protons’ has been reviewed recently [8]. Whereas in thylakoids the pattern of proton release oscillates strongly over the redox-transitions, varies as function of pH, and allows at least some discrimination between electrostatically and chemically driven events [3], in core particles it is featureless [5,6]. But as an unequivocal attribution of pH transients observed in core particles to the events at the oxygen-evolving side is more involved than in thylakoids, it is scrutinized in this article.

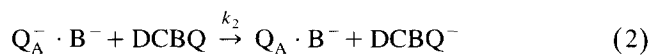
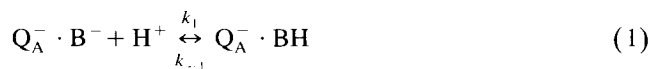
(1) *The rapid relaxation of higher S-states.* In thylakoids and in PS II enriched membrane fragments (BBY membranes) the relaxation of the higher oxidized states (S_2 , S_3) towards S_1 takes some tens of seconds up to several minutes depending on the acceptor conditions [29,30] (see also detailed studies by Messinger and Renger [31]). One consequence of the slow relaxation is, that every recording with a dark-adapted, i.e., S_1 -synchronized ensemble calls for a new sample. Core particles prepared from spinach with the detergent β -DM reveals a much

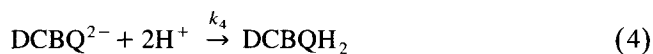
faster relaxation of the higher redox states [21,23,26]. Lifetimes of 1 and 3 s for S_2 and S_3 are published for the preparation of Van Leeuwen et al. [14], whereas the relaxation of S_0 into S_1 is reportedly still rather slow (2–3 min) [23]. Aiming at signal-to-noise improvements by averaging we asked whether repetitive dark adaptation is feasible in this material. Our preparation differed from the original one in the starting material (pea instead of spinach) and pigment content (about 100 molecules Chl per reaction centre [10] compared with 35 [14]). When exciting a core preparation (modified from pea) with a series of light flashes and monitoring the oscillations of absorption transients at a wavelength of 295 nm, which are indicative of redox transients of the manganese-containing centre, we found the same oscillation (period four) and the same damping (equivalent to $\cong 20\%$ misses) under long-term dark adaptation (20 min) and under repetitive dark adaptation (25 s). Repetitively dark-adapted core particles were well synchronized. The repetitive dark adaptation facilitated signal-averaging by saving on the amount of biological material.

(2) *The superimposition of acid-base reactions at both sides of PSII.* This was unravelled by characterizing the protonation/deprotonation of the intrinsic (Q_A , Fe) and extrinsic electron acceptors (DCBQ, hexacyanoferrate(III)).

The *preoxidation* of the non-haem iron by hexacyanoferrate(III) virtually eliminates the release of protons upon the first flash [24]. It is known from literature that the non-haem iron at the acceptor side is oxidized in the time range of minutes [24,28]. The pH-dependence of its redox potential (60 mV/pH-unit) implies the uptake of one proton per electron [32,33]. Accordingly, its rereduction upon the first flash in some tens of microseconds [34] causes extra proton uptake in a long-term dark-adapted sample, which is absent upon the following flashes. Under repetitive dark adaptation, on the other hand, the time interval between flash groups (25 s) was too short for the oxidation of the non-haem iron. Any residual small degree of oxidation of the non-haem iron under these conditions would tend to fake a slight oscillation of proton release, where there was truly none.

The analysis of the transient signals (of measurements with repetitive excitation and when the non-haem iron was not preoxidized in dark-adapted samples) in terms of only two exponentials is just phenomenological. The reactions in the presence of DCBQ were interpreted by the following reaction scheme. At the donor side of Photosystem II there was an irreversible release of 1H^+ /PS II. At the acceptor side the sequence of events was as follows:





wherein B^- denotes a buffering amino acid residue in the vicinity of Q_A .

The solid line in Fig. 5A simulates the observed behaviour at pH 5.5 of two transients, of the pH (data points in Fig. 5A) and in the near UV (not documented), with the following kinetic constants:

$$k_1 = 10^{10} \text{ M}^{-1} \text{ s}^{-1}$$

(assumed for a diffusion controlled protonation of a base in contact with bulk water [35])

$$k_{-1} = 4.74 \cdot 10^4 \text{ M}^{-1} \text{ s}^{-1}, k_2 = 1.7 \cdot 10^6 \text{ M}^{-1} \text{ s}^{-1}$$

$$\text{and } k_3 = 4 \cdot 10^8 \text{ M}^{-1} \text{ s}^{-1}.$$

With $k_{-1}/k_1 = (\text{Q}_\text{A}^- \cdot \text{B}^- / \text{Q}_\text{A}^- \cdot \text{BH}) \cdot [\text{H}^+]$ at pH 5.5 this yielded:

$$(\text{Q}_\text{A}^- \cdot \text{B}^- / \text{Q}_\text{A}^- \cdot \text{BH}) = 0.67$$

It was assumed that both the forward and backward reactions (1) were very rapid compared with reactions (2) and (3). Reaction (4) (again assumed as a diffusion controlled protonation of a base in contact with water) was also very rapid compared with reactions (2) and (3). The rate constant for the dismutation of DCBQ^- , almost diffusion controlled, was of the same order as given in the literature ($k = 6.3 \cdot 10^8 \text{ M}^{-1} \text{ s}^{-1}$ [17]). The rate constant for the reduction of DCBQ by Q_A^- was of the same order of magnitude which we observed for the reduction of hexacyanoferrate(III). This was surprising considering the very different polarities of these compounds, namely three negative charges of the hexacyanoferrate(III) complex contrasting with neutrality and only weak water solubility of DCBQ . It should be mentioned that k_2 was found to differ by a factor of 2 between various preparations, but within each preparation the linearity of the pseudo-first-order rate constant over the concentration of DCBQ was precisely met. From the foregoing it was obvious that the biphasic transient acidification following a flash of light was caused by the rapid release of 1H^+ /PS II from the donor side which was counteracted by the rapid uptake of $n\text{H}^+$ /PS II at the acceptor side with $0 < n < 1$ (e.g., at pH 5.5, $n = 0.4$). The latter was reversed upon the reduction of the added electron acceptor, giving rise to a slow phase of proton release.

(3) *The kinetic properties of proton release.* The kinetic resolution for pH-transients originating from aggregated protein as seen by pH-indicating dyes in solution is hampered by diffusion/reaction of protons in buffering domains [36,37] if the particles are aggregated. This was the case in previous experiments from our laboratory [5] with core particles prepared after Ghanotakis et al. [11]. By using a different type of core preparation [14] and by choice of the right concentration of detergent (typ. 0.01% (w/v) of β -DM), a much higher time resolution was achieved in the present work.

When scanning the rate of deprotonation upon oxidation

of the oxygen-evolving complex we found a strong variation as function of the pH. The apparent half-rise of the rapid component was shortened upon lowering of the pH (250 μs at pH 7.5, 70 μs at pH 6.0 and 12 μs at pH 5.2). According to the previous paragraph the time-course of the acidification was complex with contributions from the donor side and from the acceptor side of PS II. Even the rapid component was composite from a negative directed contribution (acidification) caused by the donor side (Y_Z and manganese) plus a positive directed contribution (alkalinization) from the acceptor side. The data showed that the contribution from the donor side was always larger. Let us consider two extreme cases. If the rise time of proton uptake is much shorter than that of proton release, the composite signal will start with a very rapid rise (alkalinization); and the following rapid decay almost truly reflects the time-course of proton release from the donor side (as observed at pH ≥ 7 , where the transients of pH started with an alkalinization, and upon the first flash in long-term dark-adapted samples). If, on the other hand, proton uptake around the quinone is slower than the release at water oxidation the composite curve should reveal a rapid acidification first which is then apparently slowed down because of its superimposition with the slower alkalinization. In this case, the apparent rate of the acidification represents a lower limit to the true one. At acid pH the alkalinization was seemingly absent, probably because both contributions were similarly rapid (e.g., 10 μs at pH 5) and experimentally unresolved. That proton uptake around the quinone binding domain can be that fast has not previously been observed. In thylakoids the shortest relaxation time was some 100 μs probably because of shielding of the Q_A -domain [27]. The time resolution by the indicator was no problem. It was checked by laser photolysis of 'caged-proton' [38]. A half-rise time of 500 ns was detected in the same set-up at pH 5.5 and with MR or BCP as pH indicators (K. Lakomiak, W. Drenstedt and W. Junge, unpublished data). According to the foregoing, the observed rate constant of the rapid acidification was in the same range of magnitude as, and perhaps lower than the true rate constant of proton release from the donor side of PS II. As the variation of this rate constant as function of pH ranged over a factor of 20, we did not worry about a possible error on a factor of 2 (simulation not documented), caused by the neglect of the superimposition of the events at both sides of PS II.

A linear relationship between the rate of deprotonation and the concentration of free protons, as observed between pH 5 and 6, is characteristic for a spontaneous deprotonation of a series of groups with spread $\text{p}K$ values in response to their exposure to a more positive electrostatic potential. The rate of deprotonation of an acid is controlled by its $\text{p}K$. If the acid is in contact with water, the on-reaction is diffusion-controlled with $k_+ \cong 10^{10} - 10^{11} \text{ s}^{-1}$ [35]; and the off-rate constant is $\text{p}K$ -controlled with $k_- \cong k_+ \cdot K$, where K denotes the dissociation constant. If

the deprotonation which is caused by the deposition of a new positive charge into the Y_Z /manganese centre electrostatically shifted the pK values of a series of acids towards acidity, the response at any pH was dominated by those acids whose newly acquired pK falls close to the given pH. The rate of proton release would then broadly increase when lowering the pH. This argument is not limited to a series of electrostatically isolated acids. It extends to a situation with many electrostatically strongly coupled acids with a series of pK values that are collective properties of this ensemble. This is fully compatible with the observed extent of proton release. An extent of precisely one proton per electron, which is independent of the pH, is expected if a group of several acids is exposed to a positive directed jump of the electric potential. If these groups interact strongly with each other the deprotonation of any particular one suppresses the deprotonation of the other groups (negative cooperativity by Coulomb force; for a discussion of these implications see also [39]).

We found no dependence of the rates of protonation/deprotonation on the chemical nature or the concentration of the pH-indicating dyes. This was at variance with the situation in thylakoid membranes where the amphiphilic pH-indicator Neutral red reacted directly with the proton donating groups because of its high concentration at the membrane surface (about 1000-fold up-concentration in the reaction volume) [3]. This again proved that the deprotonation was caused by a spontaneous protolysis into the aqueous and buffering bulk phase.

The electron transfer between the manganese cluster and Y_Z^+ occurs with half-rise times of 30, 110, 350 and 1300 μs starting with $S_0 \Rightarrow S_1$ as determined with BBY-membranes [19]. We found (80), 75, 200 and 4500 μs in our preparation [10]. At acid pH and under repetitive excitation the deprotonation in 12 μs was faster than the electron transfer in every single state transition. It occurred at the level of Y_Z^+ , as proposed previously based on work on thylakoids [3,40]. Interestingly, the extent of proton release was unchanged upon further electron transfer from manganese to Y_Z^+ . It is compatible with this observation, that the large variations of the extent of proton release as function of the pH in thylakoids influenced neither the extents nor the rates of electron transfer between the manganese cluster and Y_Z^+ [10]. This is suggestive of the positioning of both the manganese cluster and Y_Z^+ in a polar pocket of the protein.

Acknowledgements

We wish to thank our colleagues Michael Haumann and Wolfgang Drevenstedt for critical and fruitful discussion as well as Hella Kenneweg for technical assistance. This work was financially supported by the Deutsche Forschungsgemeinschaft through SFB 171-TPA2, the Land Niedersachsen and the Fonds der Chemischen Industrie.

References

- [1] Renger, G. (1993) *Photosynth. Res.* 38, 229–247.
- [2] Debus, R.J. (1992) *Biochim. Biophys. Acta* 1102, 269–352.
- [3] Haumann, M. and Junge, W. (1994) *Biochemistry* 33, 864–872.
- [4] Rappaport, F. and Lavergne, J. (1991) *Biochemistry* 30, 10004–10012.
- [5] Lübbers, K. and Junge, W. (1990) in *Current Research in Photosynthesis*, Vol. I (Baltscheffsky, M., ed.), pp. 877–880, Kluwer, Dordrecht.
- [6] Wacker, U., Haag, E. and Renger, G. (1990) in *Current Research in Photosynthesis*, Vol. I (Baltscheffsky, M., ed.), pp. 869–72, Kluwer, Dordrecht.
- [7] Lübbers, K., Haumann, M. and Junge, W. (1993) *Biochim. Biophys. Acta* 1183, 210–214.
- [8] Lavergne, J. and Junge, W. (1993) *Photosyn. Res.* 38, 279–296.
- [9] Kretschmann, H. and Witt, H.T. (1993) *Biochim. Biophys. Acta* 1144, 331–345.
- [10] Haumann, M., Bögershausen, O. and Junge, W. (1994) *FEBS Lett.* 355, 101–105.
- [11] Ghanotakis, D.F., Demetriou, D.M. and Yocum, C.F. (1987) *Biochim. Biophys. Acta* 891, 15–21.
- [12] Haag, E., Irrgang, K.D., Boekema, E.J. and Renger, G. (1990) *Eur. J. Biochem.* 189, 47–53.
- [13] Jahns, P., Haumann, M., Bögershausen, O. and Junge, W. (1992) in *Research in Photosynthesis*, Vol. II (Murata, N., ed.), pp. 333–336, Kluwer, Dordrecht.
- [14] Van Leeuwen, P.J., Nieveen, M.C., Van de Meent, E.J., Dekker, J.P. and Van Gorkom, H.J. (1991) *Photosyn. Res.* 28, 149–153.
- [15] Berthold, D.A., Babcock, G.T. and Yocum, C.F. (1981) *FEBS Lett.* 134(2), 231–234.
- [16] Junge, W. (1976) in *Chemistry and Biochemistry of Plant Pigments* (Goodwin, T.W., ed.), pp. 233–333, Academic Press, New York.
- [17] Rich, P.R. and Bendall, D.S. (1980) *Biochim. Biophys. Acta* 592, 506–518.
- [18] Dekker, J.P., Van Gorkom, H.J., Wensink, J. and Ouwehand, L. (1984) *Biochim. Biophys. Acta* 767, 1–9.
- [19] Dekker, J.P., Plijter, J.J., Ouwehand, L. and Van Gorkom, H.J. (1984) *Biochim. Biophys. Acta* 767, 176–179.
- [20] Van Leeuwen, P.J., Heimann, C., Dekker, J.P., Gast, P. and Van Gorkom, H.J. (1992) in *Research in Photosynthesis* (Murata, N., ed.), pp. 325–328, Kluwer, Dordrecht.
- [21] Van Leeuwen, P.J., Heimann, C., Kleinherenbrink, F.A.M. and Van Gorkom, H.J. (1992) in *Research in Photosynthesis* (Murata, N., ed.), pp. 341–344, Kluwer, Dordrecht.
- [22] Van Leeuwen, P.J., Van Gorkom, H.J. and Dekker, J.P. (1992) *J. Photochem. Photobiol. B: Biol.* 15, 33–43.
- [23] Van Leeuwen, P.J., Heimann, C., Gast, P., Dekker, J.P. and Van Gorkom, H.J. (1993) *Photosynth. Res.* 38, 169–176.
- [24] Renger, G., Wacker, U. and Völker, M. (1987) *Photosynth. Res.* 13, 167–184.
- [25] Renger, G. and Völker, M. (1982) *FEBS Lett.* 149, 203–207.
- [26] Gleiter, H.M., Haag, E., Inoue, Y. and Renger, G. (1993) *Photosynth. Res.* 35, 41–53.
- [27] Haumann, M. and Junge, W. (1994) *FEBS Lett.* 347 (1), 45–50.
- [28] Ikegami, I. and Katoh, S. (1973) *Plant Cell Physiol.* 14, 829–836.
- [29] Styring, S. and Rutherford, A.W. (1988) *Biochim. Biophys. Acta* 933, 378–387.
- [30] Boussac, A., Maison-Peteri, B., Vernotte, C. and Etienne, A.L. (1985) *Biochim. Biophys. Acta* 808, 225–230.
- [31] Messinger, J. and Renger, G. (1994) *Biochemistry* 33, 10896–10905.
- [32] Petrouleas, V. and Diner, B.A. (1986) *Biochim. Biophys. Acta* 849, 264–275.
- [33] Bowes, J.M., Crofts, A.R. and Itoh, S. (1979) *Biochim. Biophys. Acta* 547, 320–335.
- [34] Petrouleas, V. and Diner, B.A. (1987) *Biochim. Biophys. Acta* 893, 126–137.

- [35] Eigen, M. (1963) *Angew. Chem.* 12s, 489–588.
- [36] Junge, W. and Polle, A. (1986) *Biochim. Biophys. Acta* 848, 265–273.
- [37] Junge, W. and McLaughlin, S. (1987) *Biochim. Biophys. Acta* 890, 1–5.
- [38] Janko, K. and Reichert, J. (1987) *Biochim. Biophys. Acta* 905, 409–416.
- [39] Haumann, M. and Junge, W. (1995) in *Advances in Photosynthesis: Oxygenic Photosynthesis –The Light Reactions* (Ort, D. and Yocum, C.F., eds.), Kluwer, Dordrecht, in press.
- [40] Förster, V. and Junge, W. (1985) *Photochem. Photobiol.* 41, 183–190.